Non-vascular ceramic sherds coming from two Italian Etruscan settlements: peculiarities and interpretation of their possible use

heritage

MDPI

Article

Non-Vascular Ceramic Sherds Coming from Two Italian Etruscan Settlements: Peculiarities and Interpretation of Their Possible Use

Margherita Cantelli [1], Dafne Cimino [1], Alberta Facchi [2], Raymond J. Phaneuf [1,3] and Elisabetta Zendri [1,*]

[1] Department of Environmental Sciences, Informatics and Statistics, Ca' Foscari University of Venice, Via Torino 155, 30172 Venice, Italy; cantellim88@gmail.com (M.C.); dafne.cimino@unive.it (D.C.); phaneuf@umd.edu (R.J.P.)
[2] National Archaeological Museum of Adria, Ministry of Culture, Via Badini 59, 45011 Adria, Italy; alberta.facchi@beniculturali.it
[3] Department of Materials Science and Engineering, University of Maryland, College Park, MD 20742, USA
* Correspondence: elizen@unive.it

Abstract: Peculiar non-vascular ceramic slabs of uncertain use were found in two different Etruscan settlements of the Po Delta region (San Basilio di Ariano nel Polesine and Adria, North-East Italy) dated back to the first millennium BC. Different interpretations concerning the primary role of these fragments have been suggested by previous scholars. To bring to light an understanding of the construction processes that appear to be unique to the San Basilio and Adria settlements, a multi-analytical approach has been carried out. Macroscopic observations enabled these materials to be preliminary subdivided into groups based on chromatic features, followed by the identification of their chemical composition through FTIR-ATR spectroscopy. Moreover, the open porosity was estimated by the total water absorption test, and the superficial morphology and elemental composition of specific samples were analyzed using SEM-EDS. Furthermore, the firing temperature of a few selected fragments was evaluated by the TGA-DSC technique in order to investigate ancient production techniques. The results of the research lead us to consider the role of these peculiar non-vascular ceramic slabs as building materials due to their specific protective properties, considering the environmental conditions of the Po Delta region.

Keywords: ceramics; Etruscan; Po Delta; morphological characterization; chemical analysis; technological use; production process

Citation: Cantelli, M.; Cimino, D.; Facchi, A.; Phaneuf, R.J.; Zendri, E. Non-Vascular Ceramic Sherds Coming from Two Italian Etruscan Settlements: Peculiarities and Interpretation of Their Possible Use. *Heritage* **2022**, *5*, 1433–1448. https://doi.org/10.3390/heritage5030075

Academic Editor: Francesco Paolo Romano

Received: 19 May 2022
Accepted: 22 June 2022
Published: 26 June 2022

1. Introduction

The Etruscans were a population that lived in pre-Roman Italy during the first millennium BC, establishing a rich and thriving culture in the areas corresponding to Tuscany, Umbria, Lazio, Po Valley, Emilia-Romagna and partly Campania. In the sixth century BC, the so-called Padan Etruria, which was an area located north of the Apennines, underwent significant expansion and transformation; new settlements were established, mainly along the banks of the Po River and its delta [1,2]. The Po Delta territory became an important commercial area, trading with Etruscan, Greek, Veneti and Transalpine populations.

Concerning the architecture of housing structures, the Etruscan culture left across the hilly and plain territories of central and southern Italy clear archaeological evidence of their use of available materials: dwellings or public buildings using stone foundations and, occasionally, walls covered by stone as in the case of the site at Marzabotto, near Bologna [3]. A different situation emerged in the plain colonies in the Po Delta region, where the architecture made use of local materials such as reeds, wood and silt-clay soil [4,5].

In the second half of the last century, a branch of archaeology developed, focusing on settlements built with perishable materials; given the limited source of findings, cooperation

with archaeometry is essential for the understanding and the interpretation of data. Here, we detail an analytical study that takes up such a challenge.

The fragments analyzed in this study, which are currently stored in the warehouse of the National Archaeological Museum of Adria, were discovered during two excavation campaigns in the Po Delta area (Figure 1): the former from 1983 in San Basilio di Ariano nel Polesine (SB83) and the latter from 2015–2016 in Adria, in Via Ex Riformati (AER16) (Both excavation campaing were directed by the scientific direction of the Archaeological Superintendence under the supervision of Dr. Maurizia De Min (San Basilio) and Dr. Maria Cristina Vallicelli (Adria)).

Figure 1. Current location of the archaeological sites considered in the study; Po Delta region (north-eastern Italy) [6].

San Basilio di Ariano nel Polesine was founded near the seacoast around the end of the seventh century or the beginning of the sixth century BC. It represented not only an important harbor but also a place where different cultural and commercial entities met. Shortly afterwards, at the beginning of the sixth century BC, Adria was settled in the region between the Adige River and the main course of the Po–Tartarus River system, becoming an important fluvial commercial port and representing a central connection between the Adriatic Sea and the inland. Among others, these places were in contact with the harbor of Spina, settled during the second half of the sixth century BC, in what is now the Ferrarese branch of the Po River, which became one of the main trade centers in the Delta Region (Supplementary Materials S1, Figure S1).

The site of San Basilio revealed an inhabited context, characterized by three anthropic layers and two distinct phases [5,7], which was leveled and abandoned following a fire. Since stratigraphic units are not indicated, findings were subdivided according to the different levels of the excavation ditch. Recent excavation surveys have designated the dating back to the end of the seventh century–beginning of the sixth century and the third century BC. The site of Adria revealed a complete stratification from the first millennium BC to the medieval age. In particular, the oldest phases (sixth–fifth centuries BC) disclosed several distinct sub-phases characterized by different buildings separated by a narrow discharge ditch; more precisely, in the second phase, there was a so-called "house-workshop" dedicated to metallurgical activities [8].

In both sites (SB83 and AER16), building structures had to cope constantly with environmental conditions typical of the delta area: the presence of water and a high level of atmospheric humidity. Materials used in the construction process were local and included soil, clay, sand, wood and organic materials. The sites revealed wooden elements (burned by a fire in site SB83), rammed earth floors with burnt areas and several materials that denoted the use of wattle and daub as building techniques.

The ceramic fragments considered in this study were initially (right after the 1980s excavation) referred to as *concotto* by archaeologists, but a brief explanation is merited about the use of this term. In Italy, in the study of prehistoric and protohistoric architecture, this term is variably defined: Tasca adopts it in referring to unidentified non-vascular fragments and mixtures, found in situ or in secondary bed, subject to firing caused by their function [9]; Moffa defines *concotto* as silt-clay mixture generally underwent to fire [10]; Peinetti considers *concotto* any structural finding subject to thermal alteration in the past and found in a primary or secondary location [11]. Basically, this term is mainly used when a functional definition cannot be assigned to archaeological findings or when the morphological features cannot allow a precise interpretation of them.

In this study, we decided to use a more general terminology, such as "fragments of ceramic slabs", to avoid misunderstanding and be consistent with recent publications [8,12].

Classified as non-vascular ceramic fragments, these objects are the main subject of the present work; in particular, we seek to explore their uniqueness and their uncertain role. At SB83, they were discovered along with several samples of building materials in the abandonment strata, whereas at AER16, they were found on the ground floor of abandoned structures and the bottom of a ditch containing vertical wooden poles with a support function. Aside from San Basilio and Adria, these unusual objects were also found during the excavation on the shore of Spina, the main Etruscan settlement in the Po Delta area, some of them positioned for the lining of a pit meant to contain horizontal wooden support beams [12,13].

Aim of the Research: Archaeological Open Questions

We postulate that the fragments as found were in conditions not representing their primary use. Indeed, different interpretations have been suggested by previous scholars concerning the role of fragments of this type: building materials used for covering house walls, as external or internal plasters, calling them intonaco [13], slabs used to protect and isolate ditches holding the foundation beams [12], wall panels or parts of wattle ceilings [8].

These ceramic slabs raise a number of open questions whose answers have the potential to bring to light an understanding of construction processes that appear to be unique to the San Basilio, Adria and Spina settlements. In particular:

- Do macroscopic discrepancies in the material mean compositional differences?
- Can compositional characteristics suggest possible different uses?
- Were these slabs subjected to baking during the production process, or were they applied raw and successively exposed to a deliberate fire of the building structure?
- Since some of the fragments show a different aesthetical appearance in terms of color, is this deliberate, for a decorative effect, or the consequence of the natural deterioration of the surface?
- Perhaps most significantly, which were the main advantages of using these slabs as building materials in the Po Delta area?

The focus of this research is to address these questions using a detailed multi-analytical technique-based procedure.

2. Materials and Methods

2.1. Materials

The samples considered here have been classified as fragments or sherds since they appear to be broken off parts of a larger whole, and few of them could be assembled back together; however, none of these joints presents a specific shape that could be attributed

to a usual slab or tile. The fragments are different in size and shape (Figure 2), with a heterogeneous surface extension (10 ÷ 110 cm^2) and a non-uniform thickness of ca 1.5 cm. The two broad faces of each fragment differ in their aspect: one seems to be smoothed (hereafter called "side A"), whereas the other appears rough and irregular, in some cases also flaked (side B; Figure 3). A substantial portion of the fragments has, on side A, a repetitive groove that appears to be deep and tight for the SB83 fragments and large, flat and shallow for AER16 ones. This peculiar feature is also present in the fragments found in the excavation on the shore of Spina, and therefore it represents a distinctive aspect of the Etruscan fragments discovered in the Po Delta area. Considering this, it was decided to consider only fragments with the particular groove on side A; 70 from SB83 and 109 from AER16, out of more than 400 shards in total (Supplementary Materials S1).

Figure 2. Non-vascular ceramic fragments.

(**a**) (**b**)

Figure 3. Side A (**a**) and B (**b**) of a representative sample.

Moreover, some pieces present twisted decoration or finger impressions on one edge, taken as clear evidence of their hand-crafted production.

2.2. Morphological, Chemical and Physical Characterizations

Discrepancies between fragments visible to the naked eye were explored in detail via digital microscope observations (Dino-Lite AM4113). Surface magnification of selected samples allowed the division of slabs into groups, each with its own peculiar features. To acquire morphological information about the ceramic matrix and look for the presence of possible inclusions and/or cover layers, one representative sample for each group underwent analysis. Moieties were embedded in polyester resin and subsequently polished with a series of decreasing grit size abrasive papers to obtain cross-sections, followed by microscopic imaging using an Olympus SZX16 stereomicroscope.

To allow non-invasive and in situ preliminary investigations of sample composition, Fourier transform infrared spectroscopic analyses (FTIR) was carried out using a portable Bruker ALPHA spectrometer equipped with an attenuated total reflection (ATR) modulus based on a single-bounce diamond ATR crystal. Two representative samples for each group were placed on the crystal and directly examined without any preparation. Several spots on both the A and B faces of fragments were analyzed. Spectra were recorded in the range 4000–400 cm^{-1} with a 4 cm^{-1} resolution and an average of 32 scans. Transmission mode FTIR was instead employed to characterize the bulk composition of micro-samples of sherds judged to be significant.

The open porosity of the sherds was estimated by a total water absorption test. This was judged to be preferable to mercury intrusion porosimetry analysis because the latters' destructive character does not allow further analyses on the same sample. Furthermore, considering the object as a whole, the absorption test provides a more comprehensive result regarding ancient productions. Procedure guidelines for establishing water absorption by total immersion are detailed in NORMAL 7/81; according to that, samples should have the same shape and width to directly correlate obtained values with the volume, and should be dried in an oven at 60 °C before being weighed. For this study, a different approach has been chosen, considering that a non-destructive strategy was recommended.

After storage in a controlled indoor dry environment for 2 weeks (T = 20 ± 3 °C; HR% = 40 ± 5%), two representative samples for each group were weighed with a technical balance (resolution 0.01 g) and subsequently submerged in water and reweighed after specific periods (5, 15, 30, 45, 60, 90 and 120 min) until the achievement of a saturation level, to estimate the amount of water absorbed (*WA*) and to obtain absorption vs. immersion time curves. The amount of water absorbed (*WA*) was estimated through the following Equation:

$$WA\% = \frac{(M_t - M_i)}{M_i} \times 100$$

where M_t corresponds to the mass at a certain time t, and M_i to the initial mass of the dry sample.

Characterization of the superficial morphology and elemental composition of samples with a different aesthetical surface appearance was carried out using scanning electron microscopy and energy-dispersive X-ray spectroscopy (SEM-EDS) analyses on selected spots and areas of bare samples. Additional analyses were conducted on cross-sections of samples using a TM3000 Hitachi tabletop scanning electron microscope coupled with an X-ray microanalysis system SwiftED3000. SEM images were collected at accelerating voltages of 15 and 30 kV. EDS spectra were acquired using an accelerating voltage of 15 kV, with an acquisition time of 180.0 s and a processing time of 5 s.

2.3. Production Techniques

The ancient production techniques for these sherds were investigated in part by evaluating the effects of modern, laboratory-based heat treatment on such fragments, described below. Seven samples, representative of the different groups, were selected to be

analyzed by thermogravimetry (TG) coupled with differential scanning calorimetry (DSC). The surface and bulk of the samples were abraded, and in each case, approximately 10 mg of powder was heated in an open platinum crucible. TG and DSC analyses were carried out simultaneously with a Netzsch 409/C instrument. A single-step run was followed: it consisted of raising the temperature from 25 to 1000 °C at a heating rate of 10 °C min^{-1} in an inert atmosphere (nitrogen) at a flow rate of 80 mL min^{-1}.

3. Results

3.1. Morphological, Chemical and Physical Characterizations

Based on preliminary visual observations by the naked eye, the ceramic sherds were subdivided into nine groups (Table 1) depending on chromatic features based on standards [14]. Pieces with twisted decoration were considered as a separate group, not considering the chromatic aspect.

Table 1. Groups subdivision of SB83 and AER16.

Site	Groups	Pieces	Color (Munsell Chart Code)
SB83	A	14	Extremely heterogeneous
SB83	C1	18	Light red (2.5YR 6/6)
SB83	C2	31	Light brown (7.5YR 6/4)
SB83	G	16	Pieces presenting a twisted decoration cord on one side
AER16	1	16	Light red (2.5YR 6/6) and reddish yellow (5YR 6/6)
AER16	2	14	Light reddish-brown (2.5YR 6/4) with tones of pale yellow (2.5Y 8/2)
AER16	3	20	Pink (7.5YR 7/4) and very pale brown (10YR 7/3)
AER16	4	19	Light brownish grey (10YR 6/2) with some tones of light grey (2.5Y 7/1)
AER16	5	22	Red (2.5YR 5/6) with some tones of light reddish brown (2.5YR 6/4)
AER16	6	13	Extremely heterogeneous with efflorescence on the surface

For the photographic documentation of each representative sample please refer to Supplementary Materials S2.

Macro- and microscopic examinations allowed some general observations:

- almost all samples from groups C1, 1 and 5 appeared to have a thin reddish outward layer on side A, which was not present in the rest of the fragments. This could be interpreted as either a sort of deliberate colored finishing or as a degradation layer. Furthermore, groups 1 and 5 were considered as a single group (from now on, called 1 + 5);
- samples from groups C2, 2 and 3 seemed to have a similar surface color; therefore, groups 2 and 3 could be combined as a single group (called 2 + 3);
- groups A and 4 displayed heterogeneities in color and some dark spots, suggesting that something different should have happened compared to other fragments, such as a depositional factor or a consequence of different firing temperatures;
- the surface of group 6 fragments appeared to be covered by crystalline efflorescence, as can be seen in the images at higher magnifications (225×) (Table 2). According to the archaeological report, these samples came from the same stratigraphic units (SU 4106 and 4098) (Supplementary Materials S1, Table S2). This suggests a deposi-

tional formation of the efflorescence caused by environmental conditions more than a compositional peculiarity.

Table 2. Percentage of mass losses per temperature range.

Sample	<100 °C	100 ÷ 200 °C	200 ÷ 400 °C	400 ÷ 600 °C	>600 °C	Total Weight Loss
367BL_6 (side A)	2.4%	12.6%	1.8%	1.0%	4.5%	22.3%
367BL_6 (bulk)	1.0%	1.6%	1.3%	0.9%	1.7%	6.5%
2P_C1 (side A)	1.1%	1.7%	1.7%	0.7%	1.6%	6.8%
303Y_1 + 5 (side A)	3.0%	1.4%	2.7%	1.7%	0.9%	9.7%
309P_1 + 5 (bulk)	1.1%	0.1%	0.5%	0.7%	0.4%	2.7%
41W_A (bulk)	0.2%	0.6%	0.7%	0.4%	0.8%	2.6%
106P_G (bulk)	1.0%	0.2%	0.8%	1.9%	1.8%	5.7%

In Figure 4, images acquired with a digital microscope on selected samples are reported.

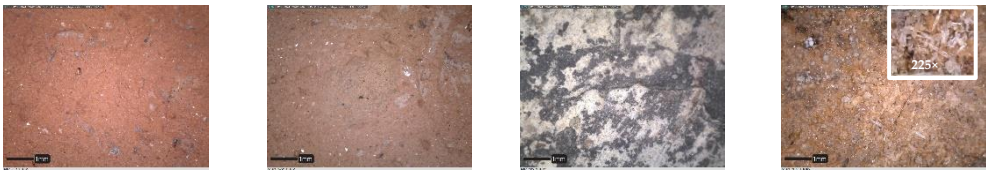

(**a**) (b) (**c**) (**d**)

Figure 4. Digital microscopic images (50×) of selected samples (side A); group C1 (**a**), group 2 + 3 (**b**), group A (**c**) and group 6 (**d**).

Four fragments were chosen, based on their features, in order to observe their polished cross-sections through a stereomicroscope, with the purpose of underlining possible differences between the ceramic bodies (Figure 5).

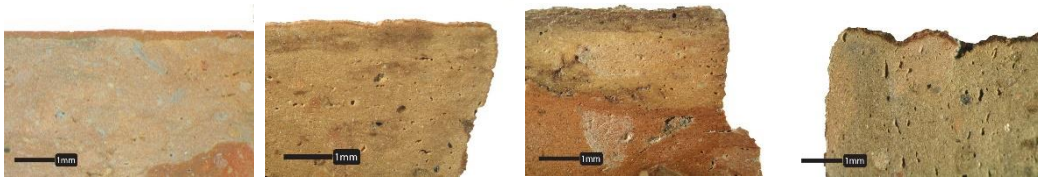

(**a**) (**b**) (**c**) (**d**)

Figure 5. Stereoscopic images (20×) of selected samples; group C1 2P (**a**), group 1 + 5 309P (**b**), group A 41W (**c**) and group 6 328BL (**d**).

Since the color of the ceramic paste depends on mineralogical composition and firing conditions, and all the samples do not present a dark ceramic paste, the presence of hematite (Fe_2O_3) can be deduced, as well as the occurrence of oxidant atmosphere during the firing process; both are factors that would cause the pinkish/reddish color of the ceramic bodies [15].

Sample 41W_A presents three stripes along the section which are different in color; this could be related to firing conditions, i.e., the sample could have been subjected to different temperatures during the manufacturing process or to a subsequent firing step causing a color change.

The thin reddish superficial layer observed by the naked eye on samples from groups C1 and 1 + 5 is evident in sample 2P_C1; however, further analysis will allow us to understand the nature of this layer (coating or degradation effect).

Sample 38BL_6 was chosen as a representative of group 6 in order to evaluate the possible presence of crystalline efflorescence in the bulk; however, it does not present morphological peculiarities.

We now consider the composition of the sherds. The FTIR-ATR spectrum of sample 303Y (side A, group 1 + 5) is shown in Figure 6, chosen as a representative for most of the ceramic artefacts analyzed.

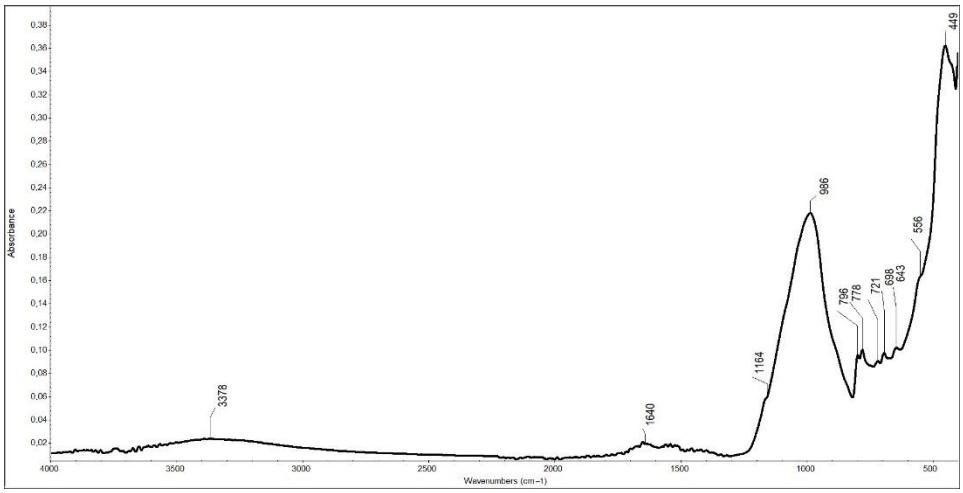

Figure 6. FTIR-ATR spectrum of 303Y_1 + 5 sample; side A, red.

Quartz (SiO_2) (peaks at 1164, 986, 796, 778, 698 and 449 cm^{-1}) [16–19] and feldspar, such as albite ($NaAlSi_3O_8$) (721 cm^{-1}) [16,20], and orthoclase ($KAlSi_3O_8$) (643 cm^{-1}) [20,21] were detected.

Evidence for iron oxides is also present in the spectra, providing some hints about firing conditions during the production of the ceramic samples. The presence of hematite (Fe_2O_3), detected in the majority of the spectra at around 556 cm^{-1}, suggests an oxidizing atmosphere in the kiln providing a red coloration to the material [19,22].

Evidence for montmorillonite ($(Na,Ca)_{0.33}(Al,Mg)_2(Si_4O_{10})(OH)_2 \cdot nH_2O$) was also detected, as broad absorption bands at 3500 ÷ 3000 cm^{-1}, centered at around 3378 cm^{-1} and 1640 cm^{-1} [18,19].

In addition, in some spectra, a peak at approximately 3624 cm^{-1} was detected, suggesting the presence of kaolinite ($Al_2(OH)_4Si_2O_5$) (Figure 7), together with three further characteristic bands (3695, 3669, 3653 cm^{-1}) typically associated with the stretching vibrations of surface hydroxyl groups [23,24].

Samples from groups A and 4 were the most heterogeneous in morphology and color based on previous observations. Sample 41W_A was chosen as the most interesting due to the layered section. The FTIR-ATR spectrum (Figure 8) includes distinct peaks which offer possible hints of the firing temperature. It does not display evidence of the presence of montmorillonite; however, it shows a weak peak at around 872 cm^{-1} related to the Fe(AlOH) group present in iron-rich clay minerals. A weak shoulder at 918 cm^{-1} ascribable to Al-Al-OH bending vibration could indicate the presence of illite [18,25] and/or kaolinite [23,26]. A peculiar characteristic of group A is also evidence of the presence of diopside ($MgCaSi_2O_6$), i.e., a peak at 504 cm^{-1} [17]: since this forms above 800 °C, its presence suggests a high temperature was reached during the production process, classifying the ceramic materials as a so-called "high-temperature crystalline phase" made of Ca-silicates [19].

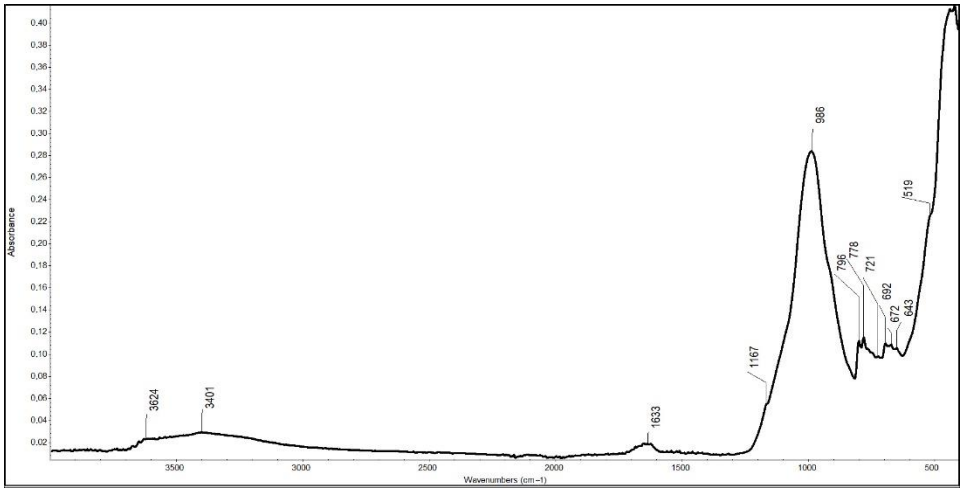

Figure 7. FTIR-ATR spectrum of 20Y_C2 sample; side B, dark spot.

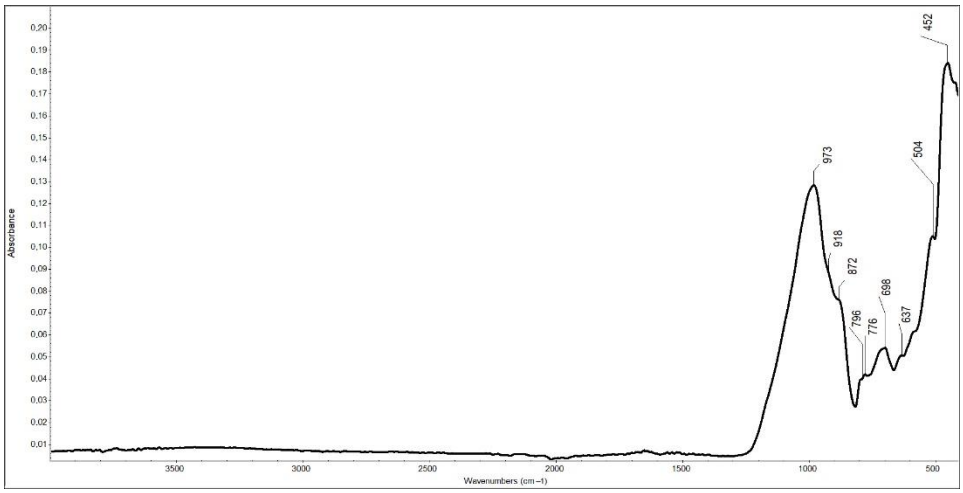

Figure 8. FTIR ATR 41W_A sample; side A, black.

The bulk of sample 41W_A was also analyzed for evidence of the presence of diopside, but FTIR revealed no signature related to it. For this sample, the presence of diopside was limited to the surface, and it might indicate that only the external part of it underwent high temperatures, i.e., possibly a consequence of the firing process related to the use of the materials.

The FTIR-ATR spectra from group 6 displayed distinctive absorption features characteristic of gypsum ($CaSO_4 \cdot 2H_2O$) at 3524, 3400, 3236, 1683, 1620, 1108, 1005, 669, 598, 441 and 419 cm^{-1}. The bulk composition of the same samples was examined in order to understand the nature and the distribution of the sulphate, previously noticed by the naked eye as crystalline efflorescence. Vibrational signs of gypsum were also detected in bulk (Supplementary Materials S3).

The open porosity of slabs was evaluated by water absorption measurements. The samples analyzed were selected based on their dimensions: only two of the larger pieces for each group were considered representative to avoid the risk of losing part of the material.

Figure 9 summarize the water absorption test results:

- three samples did not reach 15% of WA, recording the lowest values;
- most of the fragments analyzed displayed similar values, ranging from 16.7% to 22.0%.

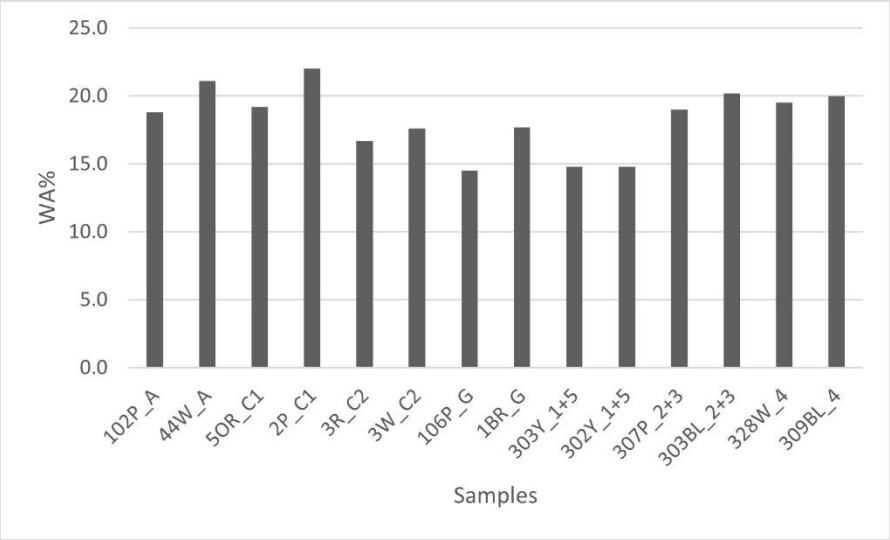

Figure 9. Water absorption values.

The absorption behavior of the sherds was monitored over time until saturation was reached (0 ÷ 120 min) and showed three general trends, observable in Figure 10.

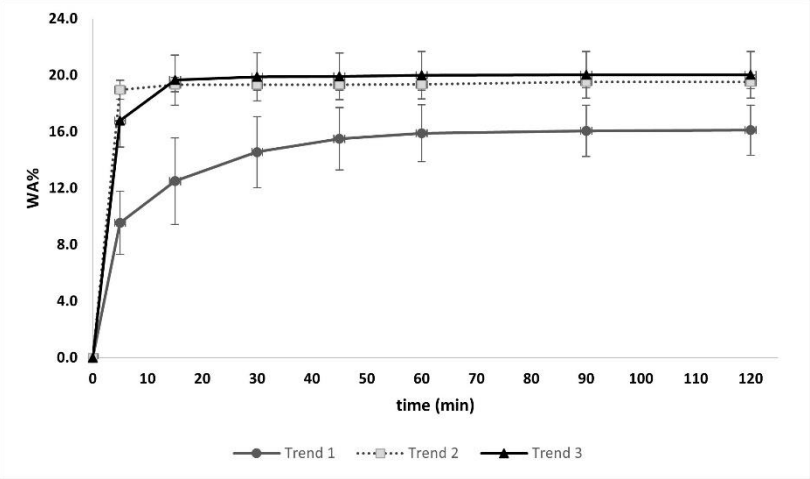

Figure 10. Water absorption trends.

For Trend 1, the water absorbed in the first 5 min was between 6% and 14%, increasing gradually until 90 min when it stabilized; for Trend 2, the major absorption occurred within the first 5 min, approximately 19%, then it reached the saturation point with limited further increase (~0.4%); Trend 3 show a higher initial absorption value, between 14% and 19% in the first 5 min, increasing by ~3% after 10 min and stabilizing until saturation (Supplementary Materials S4).

The absorption rate can hint at the size of pores: a high absorption rate suggests the presence of small pores, whereas a low rate implies bigger pores [27,28]. According to this, samples following Trend 2, characterized by a faster absorption rate, are supposed to have small pores; in contrast, samples following Trend 1 are expected to have bigger pores.

As previously observed via stereomicroscopy, most of the samples from groups C1 and 1 + 5 showed a superficial reddish finish on one side (side A). Motivated by this observation, characterization of this layer was carried out by SEM-EDX in order to evaluate the thickness, morphology and elemental composition of the layer. Two samples were chosen as representatives: 2P_C1 and 303Y_1 + 5.

As can be seen in Figure 11, the thickness of the superficial layer is not completely homogeneous. It varies between 185–210 µm for sample 2P_C1 and 65–150 µm for sample 303Y_1 + 5. In both cases, the BSE image shows different material densities between the microstructure of the upper layer and the bulk of the object, indicating a differentiation in the composition.

Based mostly on the morphology of sample 303Y_1 + 5, we postulate that the superficial layer resulted from the application of a coating which smoothed the surface.

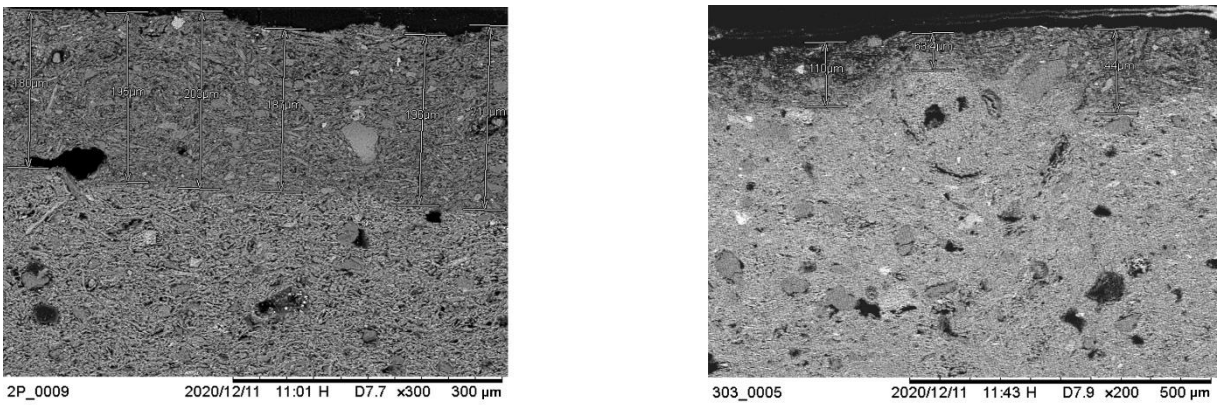

(**a**) (**b**)

Figure 11. SEM images of sample 2P_C1 (**a**) and 303Y_1 + 5 (**b**).

Turning to the elemental analysis, the presence of silicon (Si) and iron (Fe) is likely due to a non-exogenous factor, i.e., resulting from the deliberate application of a coating. Si is the main component of silicates (that are present in the sample as quartz, feldspar and clay minerals), while the Fe signal indicates the presence of iron oxides, likely in the form of hematite, which can be the main coloring agent [29]. Based on this interpretation, the ratio between these two elements was calculated to attempt to explain color differences between layers.

The weight percentage of Fe and Si was determined by EDS in the superficial layer of the two samples as well as in the bulk. Considering the Fe/Si weight ratio, in both cases, the highest values are found in the superficial layer; 1.49 in sample 2P_C1 and 2.98 in sample 303Y_1 + 5, while in the bulk, the Fe/Si ratio is 0.36 and 0.28, respectively. The compositional enrichment in the iron of the upper layer seemingly explains the chromatic difference between the bulk and the superficial side of the fragments from groups C1 and 1 + 5.

3.2. Production Techniques

Based on the previous results, seven selected samples were chosen for thermal analysis to attempt to evaluate the firing temperatures (Supplementary Materials S5).

Figures 12 and 13 show the TG-DSC thermograms related to samples 309P_1 + 5 and 303Y1 + 5, chosen as representative for the bulk and side A, respectively. They both display a broad endothermic peak between 550 and 650 °C ascribable to the loss of hydroxyl water by clay minerals [30,31]; the occurrence of this transition suggests a firing temperature lower than 500 °C.

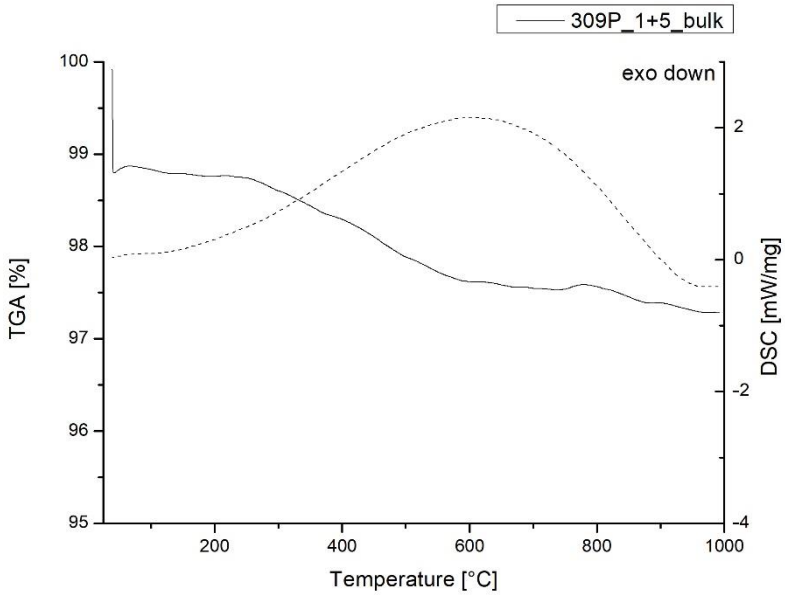

Figure 12. TG-DSC thermogram of sample 309P_1 + 5_bulk (DSC curve dotted).

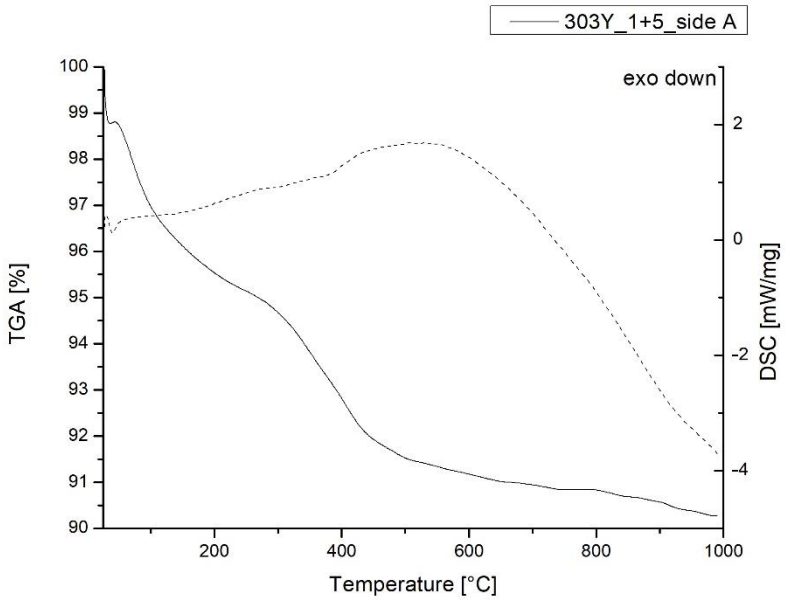

Figure 13. TG-DSC thermogram of sample 303Y_1 + 5_side A (DSC curve dotted).

In addition, with the aim of investigating the presence of gypsum in fragments from group 6, both the bulk and side A surface of sample 367BL_6 were analyzed, with results shown in the thermogram in Figure 14. It showed a sharp endothermic DSC peak at 140 °C, corresponding to the loss of water (12.6%) due to the presence of gypsum mainly on the surface. The weak shoulder at 342 °C along the DSC curve of side A can be related to water loss in iron hydroxides [31].

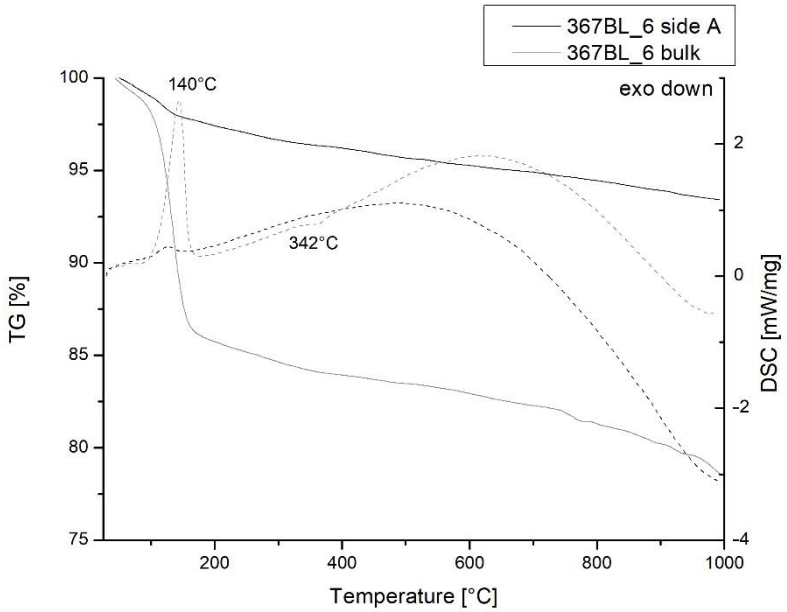

Figure 14. TG-DSC thermogram of sample 367BL_6 (side A black line, bulk grey line; DSC curves dotted).

Based on previous studies concerning the use of the TG method for the determination of the firing temperature of ceramic materials [32,33], TG results are expressed in Table 2 as a percentage of mass loss considering different temperature ranges and as total weight loss in order to compare all the samples analyzed.

A significant feature was detected in sample 367BL_6, which showed the highest total loss (22.3%), suggesting a clear difference in composition: indeed, it is characteristic of the presence of gypsum (mass loss 12.6%) detected between 100 and 200 °C.

Taken as a whole, the thermal behavior of the non-vascular ceramic sherds appeared to be qualitatively similar, even if the weight loss values differ. These latter values could not be directly correlated to the firing production process but are likely instead due to a depositional factor, possibly associated with the fact that the fragments were buried in different strata.

4. Discussion

The present work has allowed insights into important aspects of Etruscan building technology concerning the sites of San Basilio and Adria in the Po Delta region (North-East Italy). The composition of ceramic mixtures, as well as the variation in the composition of fragments from the bulk to the surface, prompt some interesting deductions about the construction processes used at these sites, including the methodology of firing and the use of coatings.

On the basis of the results obtained, it is possible to address the open questions outlined in the introduction.

- The first two questions refer to the compositional features: Do macroscopic discrepancies mean compositional differences? Can compositional characteristics suggest possible different uses?

From the macroscopic point of view, the shapes of the ceramic findings appear insignificant: even if these fragments seem to be broken off parts of a larger whole, and few of them were assemblable back together, clear-cut profiles were not detected.

Despite chromatic differentiation, the majority of the samples present as main components silicates, clay minerals and hematite, defining them as clayed materials produced from non-calcareous clay. The only macroscopic discrepancy that reveals a peculiarity in the composition is the superficial presence of crystalline efflorescence on some slabs, indicating the presence of gypsum that is related to a depositional factor.

- The subsequent question concerns the firing process: Were they subjected to baking during the production process, or were they applied raw and successively exposed to a deliberate fire of the building structure?

The spectroscopic results for some samples from groups 4 and A display the presence of diopside, a mineral generally formed above 800 °C, only on the superficial side, suggesting a high-temperature firing process. Aside from this, ceramic samples do not show evidence of inhomogeneous firing, and TG-DSC results indicate that all ceramic samples were produced below 500 °C.

- Another question refers to the superficial chromatic aspect of some slabs: Since some of the fragments show a different aesthetical appearance in terms of color, is this a deliberate effect or the consequence of the natural deterioration of the surface?

Some samples present a thin reddish superficial layer rich in iron which could be evidence for the application of a coating with a decorative purpose. Therefore, more doubts take shape; some scholars [12] suggested the principal use of these slabs as protection for ditches holding the foundation beams of the building structure, but if their primary place was to be underground in the foundation, why treat them with a colored engobe? We suggest that it is more likely that they were produced to be part of the unburied building materials.

- The last question to be addressed is, perhaps, the most significant: What were the main advantages of using these slabs as building materials in the Po Delta area?

Low water absorption values, such as those of the ceramic fragments studied here, imply good resistance to the natural environment and a good permeability [34]. In fact, the Po Delta area was characterized by a high level of relative humidity and abundant presence of water. The results of this study lend support to the interpretation of the use of these non-vascular ceramic fragments as building materials with specific, desired waterproof properties.

5. Conclusions

The results of our combined multi-analytical technique approach allow some interesting deductions about the function of Etruscan non-vascular ceramic slabs found in the Po Delta region. The chemical investigation of these indicates that some of them were apparently intentionally covered with a sort of thin reddish engobe, advancing the hypothesis of a decorative use of the material. Based on the evaluation of heat treatment, it can be assumed that the fragments were fired below 500 °C during the production process. Most significantly, the moderate water absorption values of the ceramic samples advance the interpretation as building materials with desired protective properties, in line with the environmental characteristic of the Po Delta region.

It is believed that the results of this study could be useful for future excavations in terms of enlightening the functional aspect of these materials as well as their primary location.

Supplementary Materials: The following supporting information can be downloaded at: https://www.mdpi.com/article/10.3390/heritage5030075/s1, Figure S1: The ancient Po Delta with the Etruscan settlements of S. Basilio, Adria and Spina; Figure S2: FTIR-ATR spectrum of 323W_6 sample; side A; Figure S3: FTIR spectrum of 367BL_6 sample; bulk; Figure S4: Water absorption curves: Trend 1; Figure S5: Water absorption curves: Trend 2; Figure S6: Water absorption curves; Trend3; Figure S7: TG-DSC thermogram of sample 106P_G_bulk; Figure S8: TG-DSC thermogram of sample 2P_C1_side A; Figure S9: TG-DSC thermogram of sample 41W_A_bulk; Table S1: Samples tag and strata description, SB83 site; Table S2: Samples tag and US description, AER16 site; Table S3: SB83 groups subdivision; Table S4: AER16 groups subdivision.

Author Contributions: Conceptualization, M.C., R.J.P., A.F. and E.Z.; investigation, M.C.; resources, E.Z. and A.F.; data curation, M.C. and D.C.; writing—original draft preparation, M.C., A.F. and E.Z.; writing—review and editing, M.C., R.J.P., D.C. and E.Z.; supervision, E.Z. All authors have read and agreed to the published version of the manuscript.

Funding: This research received no external funding.

Institutional Review Board Statement: Not applicable.

Informed Consent Statement: Not applicable.

Data Availability Statement: Not applicable.

Acknowledgments: The authors would like to thank Maria Cristina Vallicelli (Soprintendenza Archeologia, Belle Arti e Paesaggio per l'area Metropolitana di Venezia e le province di Belluno, Padova e Treviso), Silvia Paltineri (University of Padua), Sandra Bedetti and Leonardo Di Simone (National Archaeological Museum of Adria) for the collaboration, the technical support and the access to the archaeological documentation. The authors also thank Giulia Moro (Department of Molecular Sciences and Nanosystems, Ca' Foscari University) for the SEM analyses and the working group of the Department of Environmental Science, Informatics and Statistics of Ca' Foscari University of Venice. The authors would like to thank the Patto per lo Sviluppo della Città di Venezia (Comune di Venezia) for their support in the research.

Conflicts of Interest: The authors declare no conflict of interest.

References

1. Facchi, A. Adria. La città etrusca che ha dato il nome al Mar Adriatico. In *Etruschi. Viaggio Nelle Terre dei Rasna, Catalogo Della Mostra (Bologna, 7 Dicembre 2019–24 Maggio 2020)*; Electa: Milano, Italy, 2019; pp. 419–422.
2. Govi, E. L'Etruria padana. In *Etruschi. Viaggio Nelle Terre Dei Rasna. Catalogo Della Mostra (Bologna, 7 Dicembre 2019–24 Maggio 2020)*; Electa: Milano, Italy, 2019; pp. 357–362.
3. Govi, E.; Sassatelli, G. *Marzabotto. La Casa 1 della Regio IV—Insula 2. 1. Lo Scavo*; Ante Quem: Bologna, Italy, 2010.
4. Casini, S.; De Marini, R.C. La città etrusca del Forcello. In *L'abitato Etrusco del Forcello di Bagnolo S. Vito (Mantova): Le Fase Arcaiche*; De Marini, R.C., Rapi, M., Eds.; Tipografia Latini: Firenze, Italy, 2007; pp. 35–49.
5. De Min, M. L'abitato arcaico di S. Basilio di Ariano Polesine. In *L'antico Polesine: Testimonianze Archeologiche e Paleoambientali; Catalogo Delle Esposizioni di Adria e di Rovigo, Febbraio–Novembre 1986*; Museo Archeologico di Adria: Adria, Italy, 1986; pp. 171–184.
6. Google Maps. 2021. Available online: https://www.google.com/maps/@44.9893084,12.1826729,10z/data=!5m1!1e4 (accessed on 9 April 2021).
7. De Min, M. L'abitato arcaico di S. Basilio. In *Etruschi a Nord del po*; Campanotto Editore: Lombardia, Italy, 1988; pp. 84–91.
8. Bonomi, S.; Vallicelli, M.C.; Balista, C. The etruscan settlement of Adria (Italy–Rovigo): New data from the excavations in Via Ex Riformati (years 2015–2016). In *Crossing the Alps—Early Urbanism between Northern Italy and Central Europe (900–400 BC)*; Zamboni, L., Fernández-Götz, M., Metzner-Nebelsick, C., Eds.; Sidestone Press: Leiden, The Netherlands, 2020; pp. 193–206.
9. Tasca, G. Intonaci e concotti nella preistoria: Tecniche di rilevamento e problemi interpretativi. In *Introduzione All'archeologia Degli Spazi Domestici*; Comune di Como: Como, Italy, 1998; pp. 77–87.
10. Moffa, C. L'organizzazione dello spazio sull'acropoli di Broglio di Trebisacce. In *Grandi Contesti e Problemi Della Protostoria Italiana*; All'Insegna del Giglio: Firenze, Italy, 2002; pp. 19–31.
11. Peinetti, A. Analisi tecnologica di resti strutturali in terra: Variabilità delle tecniche di costruzione e osservazioni in sezione levigata per la caratterizzazione di concotti e conglomerati architettonici. *IpoTESI di Preist.* **2016**, *8*, 103–138. [CrossRef]
12. Cappuccini, L.; Mohr, M. Strutture a Spina nel IV sec. a. C. In *Spina—Neue Perspektiven der Archäologischen Erforschung*; Tagung an der Universität Zürich 4./5. Mai 2012; Verlag Marie Leidorf GmbH: Zurigo, Switzerland, 2017; pp. 21–26.
13. Zamboni, L. *Spina Città Liquida: Gli Scavi 1977–1981 Nell'abitato e i Materiali Tardo-Arcaici e Classici*; VML Verlag Marie Leidorf: Rahden, Germany, 2016.
14. Munsell Color Company. *Munsell Soil Color Charts (Year 2000 Revised Washable Edition)*; Munsell Color Company: New Windsor, NY, USA, 2000.
15. Cuomo di Caprio, N. *Ceramica in Archeologia 2: Antiche Tecniche di Lavorazione e Moderni Metodi di Indagine*; L'Erma di Bretschneider: Roma, Italy, 2007.
16. Akyuz, S.; Akyuz, T.; Basaran, S.; Bolcal, C.; Gulec, A. Analysis of ancient potteries using FT-IR, micro-Raman and EDXRF spectrometry. *Vib. Spectrosc.* **2008**, *48*, 276–280. [CrossRef]
17. De Benedetto, G.E.; Laviano, R.; Sabbatini, L.; Zambonin, P. Infrared spectroscopy in the mineralogical characterization of ancient pottery. *J. Cult. Herit.* **2002**, *3*, 177–186. [CrossRef]
18. Müller, C.M.; Pejcic, B.; Esteban, L.; Piane, C.D.; Raven, M.; Mizaikoff, B. Infrared Attenuated Total Reflectance Spectroscopy: An Innovative Strategy for Analyzing Mineral Components in Energy Relevant Systems. *Sci. Rep.* **2014**, *4*, 6764. [CrossRef] [PubMed]
19. Ravisankar, R.; Kiruba, S.; Eswaran, P.; Senthilkumar, G.; Chandrasekaran, A. Mineralogical Characterization Studies of Ancient Potteries of Tamilnadu, India by FT-IR Spectroscopic Technique. *E-J. Chem.* **2010**, *7*, S185–S190. [CrossRef]
20. Annamalai, G.R.; Ravisankar, R.; Naseerutheen, A.; Chandrasekaran, A.; Rajan, K. Application of various spectroscopic techniques to characterize the archaeological pottery excavated from Manaveli, Puducherry, India. *Optik* **2014**, *125*, 6375–6378. [CrossRef]

21. Ramasamy, V.; Suresh, G. Mineral characterization and crystalline nature of quartz in Ponnaiyar River sediments, Tamilnadu, India. *Am. J. Sci. Res.* **2009**, *4*, 103–107.
22. Velraj, G.; Janaki, K.; Musthafa, A.M.; Palanivel, R. Spectroscopic and porosimetry studies to estimate the firing temperature of some archaeological pottery shreds from India. *Appl. Clay Sci.* **2009**, *43*, 303–307. [CrossRef]
23. Djomgoue, P.; Njopwouo, D. FT-IR Spectroscopy Applied for Surface Clays Characterization. *J. Surf. Eng. Mater. Adv. Technol.* **2013**, *3*, 275–282. [CrossRef]
24. Madejová, J. FTIR techniques in clay mineral studies. *Vib. Spectrosc.* **2003**, *31*, 1–10. [CrossRef]
25. Alver, B.E.; Dikmen, G. Investigation of the Influence of Heat Treatment on the Structural Properties of Illite-Rich Clay Mineral Using FT-IR, 29Si MAS NMR, TG AND DTA Methods. *Anadolu Univ. J. Sci. Technol. Appl. Sci. Eng.* **2016**, *17*, 823–829. [CrossRef]
26. Ricci, G.; Caneve, L.; Pedron, D.; Holesch, N.; Zendri, E. A multi-spectroscopic study for the characterization and definition of production techniques of German ceramic sherds. *Microchem. J.* **2016**, *126*, 104–112. [CrossRef]
27. Gane, P.A.C.; Ridgway, C.J.; Schoelkopf, J. Absorption Rate and Volume Dependency on the Complexity of Porous Network Structures. *Transp. Porous Media* **2004**, *54*, 79–106. [CrossRef]
28. Ridgway, C.J.; Gane, P.A. Correlating pore size and surface chemistry during absorption into a dispersed calcium carbonate network structure. *Nord. Pulp Pap. Res. J.* **2006**, *21*, 563–568. [CrossRef]
29. Caner, E.; Güney, B.A. Characterization of ceramic ware fragments from Aizanoi-Turkey by micro Raman, XRPD and SEM-EDX spectrometry. *Spectrochim. Acta Part A Mol. Biomol. Spectrosc.* **2017**, *177*, 135–139. [CrossRef] [PubMed]
30. Leach, F.; Davidson, J.; Claridge, G.; Ward, G.; Craib, J. The Physical and Mineralogical Characteristics of Pottery from Mochong, Rota, Mariana Islands. In *Islands of Inquiry: Colonisation, Seafaring and the Archaeology of Maritime Landscapes*; ANU Press: Camberra, Australia, 2008; pp. 435–452. [CrossRef]
31. Moropoulou, A.; Bakolas, A.; Bisbikou, K. Thermal analysis as a method of characterizing ancient ceramic technologies. *Thermochim. Acta* **1995**, *269–270*, 743–753. [CrossRef]
32. Bakolas, A.; Biscontin, G.; Moropoulou, A.; Zendri, E. Physico-chemical characteristics of traditional mortars in Venice. *Trans. Built Environ.* **1995**, *15*, 187–194. [CrossRef]
33. Singh, P.; Sharma, S. Thermal and spectroscopic characterization of archeological pottery from Ambari, Assam. *J. Archaeol. Sci. Rep.* **2016**, *5*, 557–563. [CrossRef]
34. Aouba, L.; Bories, C.; Coutand, M.; Perrin, B.; Lemercier, H. Properties of fired clay bricks with incorporated biomasses: Cases of Olive Stone Flour and Wheat Straw residues. *Constr. Build. Mater.* **2016**, *102*, 7–13. [CrossRef]